IOPscience iopscience.iop.org

Home Search Collections Journals About Contact us My IOPscience

Determination of structure in liquid solutions - implications for picosecond photoexcitation studies

This article has been downloaded from IOPscience. Please scroll down to see the full text article.

2003 J. Phys.: Condens. Matter 15 S137

(http://iopscience.iop.org/0953-8984/15/1/317)

View the table of contents for this issue, or go to the journal homepage for more

Download details:
IP Address: 171.66.16.97
The article was downloaded on 18/05/2010 at 19:23

Please note that terms and conditions apply.

INSTITUTE OF PHYSICS PUBLISHING JOURNAL OF PHYSICS: CONDENSED MATTER

J. Phys.: Condens. Matter **15** (2003) S137–S143 PII: S0953-8984(03)54773-7

Determination of structure in liquid solutions—implications for picosecond photoexcitation studies

A Plech[1,3], R Randler[1], M Wulff[1], F Mirloup[2] and R Vuilleumier[2]

[1] ESRF, BP 220, F-38043 Grenoble, Cedex, France
[2] Laboratoire de Physique Theorique des Liquides, Universite Pierre et Marie Curie, 4, Place Jussieu, F-75005 Paris, France

Received 15 October 2002
Published 16 December 2002
Online at stacks.iop.org/JPhysCM/15/S137

Abstract

Solution scattering from iodine in different solvents is used to derive the cross-correlation between iodine and the solvent. In parallel, molecular dynamics simulations are performed and the findings compared to the experimental results. The close correspondence shows that it is possible to describe the structural rearrangements of the solvent around a solute molecule. Time-resolved studies of photoexcited molecules will therefore allow one to study the relaxations of the solute as well as the solvent molecules.

1. Introduction

The first structural studies of photoexcited molecules with picosecond resolution were performed using electron scattering [1]. Several limitations such as the small penetration depth in condensed matter and the limited brilliance from pulsed electron sources make it advantageous to use x-ray scattering. X-rays offer the advantage of allowing study of molecules not only in the gas phase but also in the condensed phase which give access to many rich phenomena. Present high-brilliance synchrotron and future x-ray laser sources offer a challenging potential for picosecond and subpicosecond time resolution on a wide range of systems. Encouraging model studies have already been reported [2, 3].

The principle of such an experiment is the excitation of photoactive species by a (femtosecond) laser, which is synchronized to the x-ray pulses delivered from a synchrotron or a plasma source. The short x-ray pulses probe the structural rearrangement induced by the laser after a fixed time delay. From the scattering yield the molecular structure is reconstructed. In practice these experiments are designed as pump–probe set-ups, where the scattering from a large number of pulses is accumulated and compared to the scattering of the system in the dark state.

[3] Present address: Fachbereich Physik der Universität Konstanz, Universitätsstrasse 10, D-78457 Konstanz, Germany.

0953-8984/03/010137+07$30.00 © 2003 IOP Publishing Ltd Printed in the UK

2. Materials and methods

2.1. Scattering set-up

The liquid solution is prepared in a thin-wall capillary under a steady flow from a syringe pump (0.2 m s^{-1}). Borosilicate capillaries of 300 μm diameter (Hilgenberg, Germany) are exposed to an x-ray beam of 0.1 $\times$ 0.1 mm^2 size. The energy is set to 17.0 keV by an Si(111) monochromator. The scattering is recorded by means of a MarCCD (Mar Research, Germany) fibre-coupled scintillator CCD. The accessible range of momentum transfer $Q = 4\pi/\lambda \sin(2\theta/2)$ is restricted to about 8.5 $Å^{-1}$. Additionally, the forward region 0–0.35 $Å^{-1}$ is shadowed by a beam stop for the transmitted beam. Details of the set-up at the beam station ID09B at ESRF are described e.g. in [4, 5].

The data are corrected for air and capillary scattering, detector efficiency, space–angle conversion, polarization and absorption.

The temperature of the sample was kept at 300 K (Oxford Cryostream, UK) and a careful alignment of all distances was achieved with a precision of 50 μm. Data for the solutions and their pure solvents were taken alternately in order to eliminate drifts and instabilities. The solvents (CCl_4, CH_2Cl_2, C_2H_5OH, spectroscopic grade, Aldrich) were used as received, to prepare solutions of 0.0065–0.050 mol I_2 l^{-1}.

2.2. X-ray scattering

Scattering from a liquid solution can be described in terms of the statistical pair correlation of the scattering sites [6, 7]. In order to extract the solute–solvent term it is convenient to express the total scattering $I(Q)$ as a sum over different contributions depending on the origin of the scattering centres:

$$I(Q) = I_{\mathrm{I-I}}(Q) + I_{\mathrm{I-solvent}}(Q) + I_{\mathrm{solvent-solvent}}(Q) + I_{\mathrm{solvent,excess}}(Q). \tag{1}$$

The contribution of the iodine molecular factor $I_{\mathrm{I-I}}(Q)$ is modelled by the Debye equation assuming a fixed bond length r_x of the ground state together with a Debye–Waller factor allowing for mean displacements Δr from the equilibrium distance:

$$I_{\mathrm{I-I}}(Q) = f_{\mathrm{I}}^2(Q)\left[1 + \frac{\sin Qr_x}{Qr_x} \mathrm{e}^{-\Delta r^2 Q^2}\right], \tag{2}$$

$f(Q)$ being the atomic scattering function [8]. In a set-up without energy discrimination, additional inelastic scattering is included following the Compton scattering parameters in [9]. The quantity $I_{\mathrm{solvent-solvent}}(Q)$ is the well known scattering from the pure solvent which normally dominates by far over all other contributions at the present concentrations of I_2. The small contribution $I_{\mathrm{solvent,excess}}(Q)$ will stem from the excess structure change within the solvent correlation caused by the mere presence of a solute molecule and/or by change in the liquid structure due to energy transfer from the excited iodine to the solvent. In practice it is not possible to separate this contribution, so it will be incorporated in the cross-correlation below. In the case of excitations in the solvent such as pressure waves or heating, it has to be evaluated independently.

We will now concentrate on the cross-correlation term $I_{\mathrm{I-solvent}}(Q)$: the contribution from solute molecules and the solvent environment. As the positions of pairs of iodine and solvent atoms are not fixed but described by a distribution of distances, the correlation is described by a site–site correlation function $g(r)$. The partial structure factors $H_{\alpha\beta}(Q)$ are then obtained via the Fourier transformation of the partial correlation functions $g_{\alpha\beta}(r) = (\rho(r) - \rho_\infty)/\rho_\infty$

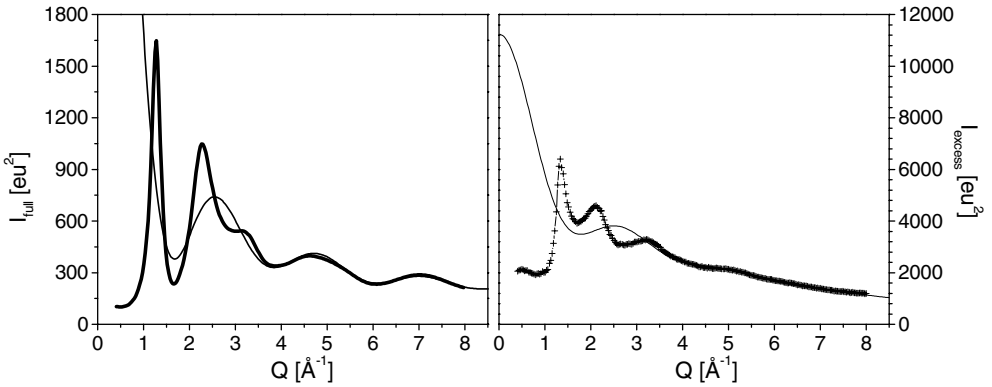

Figure 1. Scaling of the scattering cross-section to absolute units. Left: scaling of the full corrected scattering to the gas scattering of CCl_4 at high Q-values. Right: scaling of the difference between the iodine–CCl_4 solution and pure CCl_4 to the expected gas scattering of one iodine molecule.

of pairs of atomic species $\alpha\beta$:

$$H_{\alpha\beta} = 4\pi \int_0^\infty r^2(g_{\alpha\beta}(r) - 1)\frac{\sin Qr}{Qr}\,\mathrm{d}r \tag{3}$$

which are finally weighted by the concentrations and scattering factors for the atom pairs to give the scattering intensity.

The data were processed in several steps, the first of which was to scale the corrected full scattering $I(Q)$ to the gas scattering of one CCl_4 molecule to express the data in electron units; the gas scattering of CCl_4 was calculated analogously to equation (2)—as a sum of elastic and inelastic scattering. Secondly, the difference between the solution scattering and that in the pure solvent was scaled such that the difference oscillated around the calculated iodine gas scattering at high Q[4].

In figure 1 we demonstrate the scaling of the measured $I(Q)$ to the gas scattering of CCl_4 (left-hand side) and the solution minus solvent difference to the gas scattering of I_2 (right-hand side).

In order to derive the kernel of the structure function $H_{\mathrm{I-Cl(C)}}$, the iodine gas scattering is subtracted from the result and the data are finally normalized by the atomic scattering functions of iodine and the solvent scattering site. As the solvent consists of several scattering centres and only one independent measurement is possible with nonresonant x-ray scattering, it is not possible to separate individual correlation functions. In fact, the accessible $g(r)$ is a weighted sum of I–Cl and I–C components in the case of CCl_4. On the other hand, for the halogenated solvents the I–Cl correlation is dominant due to the larger number of electrons. The effective $g(r)$ function can be derived by Fourier inversion following the approach of Warren [6] with a convergence factor to reduce the effect of the finite Q-range.

2.3. Molecular dynamics simulation

Theoretical liquid form factors were obtained by molecular dynamics (MD) simulations [10]. Model pair potentials were used to describe the solvents, the I_2 molecules and their interactions. The solvent CCl_4 and CH_2Cl_2 molecules were modelled as rigid sites: five sites (C, 4 × Cl)

[4] Other direct intensity scaling procedures would require high-precision flux calibration and knowledge of the excess mixing volume etc.

Table 1. Potential parameters.

	CCl_4	CH_2Cl_2
r_{C-Cl} (Å)	1.769	1.772
r_{Cl-Cl} (Å)	2.89	2.924
σ_{CC} (Å)	3.8	3.96
σ_{ClCl} (Å)	3.47	3.35
σ_{CCl} (Å)	3.6354	3.665
q_C (e)	0.248	0.302
q_{Cl} (e)	−0.062	−0.151
ϵ_{CC} (K)	25.19	70.5
ϵ_{ClCl} (K)	134.01	173.5
ϵ_{CCl} (K)	58.10	110.6

for CCl_4 and three sites (CH_2, Cl, Cl) for CH_2Cl_2 respectively. The pair potentials describing the interactions between sites are based on Coulomb interaction with partial charges assigned to each site and a Lennard-Jones 6–12 potential of the form

$$V_{LJ}(r) = 4\epsilon\left(\frac{\sigma^{12}}{r^{12}} - \frac{\sigma^6}{r^6}\right). \tag{4}$$

We have used Jorgensen's OPLS parameters [11] for CCl_4 and the parameters of Ferrario *et al* [12] were used for CH_2Cl_2. These parameters and the geometry of the solvent molecules are summarized in table 1.

In simulations with iodine, the intramolecular I–I distance was allowed to vary with an intramolecular Morse potential from Nesbitt and Hynes [13]:

$$V_{Morse}(r) = D_e(1 - e^{-b(r-r_e)})^2, \tag{5}$$

with $D_e = 12\,547\ cm^{-1}$, $b = 1.91\ Å^{-1}$ and $r_e = 2.67$ Å. No partial charges were assigned to the iodine atoms and their interactions with the solvent sites were reduce to Lennard-Jones potentials constructed using the Lorentz–Berthelot rules, $\sigma_{AB} = (\sigma_{AA} + \sigma_{BB})/2$ and $\epsilon_{AB} = \sqrt{\epsilon_{AA}\epsilon_{BB}}$ for the interaction between sites A and B. The values $\sigma_{II} = 3.8$ Å and $\epsilon_{II} = 240$ K were determined by Bergsma *et al* [14] from a fit of the I–Ne and I–He interactions.

The pure solvents were simulated with 256 molecules at the experimental densities. One iodine molecule was then inserted keeping the volume of the cell fixed. We consistently used periodic boundary conditions (with Ewald summation for the electrostatics) and a velocity Verlet integrator along with the SHAKE/RATTLE algorithm [15] to keep the solvent molecules rigid. A time step of 1 fs was used and averages were taken over 1 ns.

Work on simulations for ethanol is currently in progress.

3. Results and discussion

We present the scattering cross-sections for the liquids CCl_4, CH_2Cl_2 and CH_3CH_2OH which act on the iodine recombination very differently [16, 17]. These solvents span a range of different electron densities and they have different cross-correlation perturbations [14]. Iodine in CCl_4 has the longest lifetime for the cooling of vibrationally excited molecules and geminate A/A′ relaxation to ground state, which is explained by the slow energy transfer to the solvent and probably also by structural cage effects. On switching to CH_2Cl_2, the relaxation times are reduced by more than a factor of 2. Low-n alcohols such as ethanol on the other hand are known to have extremely short lifetimes. In addition, they form a charge transfer state with I_2 which should be associated with structural rearrangement. In figure 2 the partial structure functions

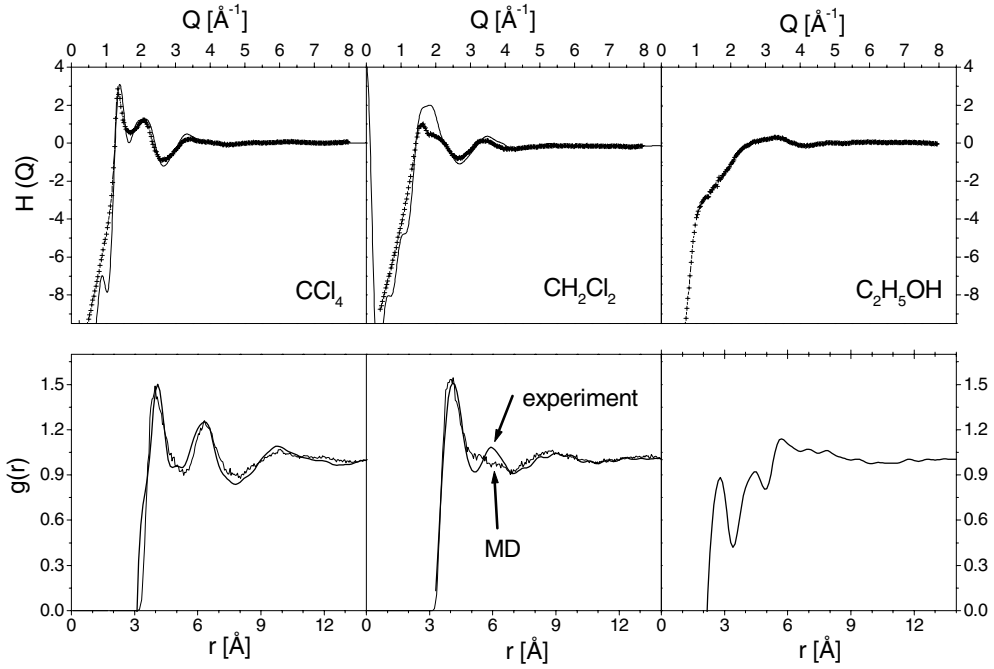

Figure 2. Partial structure factors of the iodine–solvent correlation for the different solvents (upper panel). The crosses represent the experimental data; the full lines represent the MD simulation. The corresponding effective $g(r)$ is plotted below for the back-transform as well as $g_{\mathrm{I-Cl}}(r)$ from the MD simulation. The iodine concentration was 50 mM.

$H_{\mathrm{I-solvent}}$ are displayed together with the effective pair distribution functions. Experimental data are compared with the results from MD simulation. It is clear that the structure function of the I_2 gas scattering is strongly perturbed in the low-Q region as well as at distinct values where peaks are formed. From the correlation function one can deduce clear peaks for the nearest-neighbour and next-nearest-neighbour distances. The strongest structuring is observed for CCl_4 which has the most rigid packing. For ethanol, only the cavity formed by I_2 is visible, with hardly any visible packing of radial symmetry.

We find that the iodine–iodine distance is relaxed from the value $r_x = 2.66$ Å in the gas phase to 2.70–2.72 Å in solution. This can also be observed in the cross-correlation next-neighbour peaks, which are shifted in comparison to those from an MD simulation that has been performed with 2.66 Å bond length. Termination errors of the back-transform and MD finite-size effects limit the discussion of the density of packing, as seen from the peak shapes.

In practice, the cross-correlation scattering masks the iodine scattering in part. This makes it more difficult to derive the parameters of the structural changes of the solute after photoexcitation. For example, from the gas scattering it would be possible to extract information about bond breaking from the intensity change in the forward direction, which gives the number of coherent scattering electrons. On the other hand, the high-Q scattering does not differ substantially from gas scattering. This region can therefore act as a reference for separating intramolecular and intermolecular changes. We calculate the difference in scattering of photoexcited iodine in CCl_4 in figure 3. In this case the MD simulation of the extended A/A′ state with a bond length of 3.15 Å is used to simulate the difference in intensity between the laser-excited and dark states scaled to electron units of one iodine molecule.

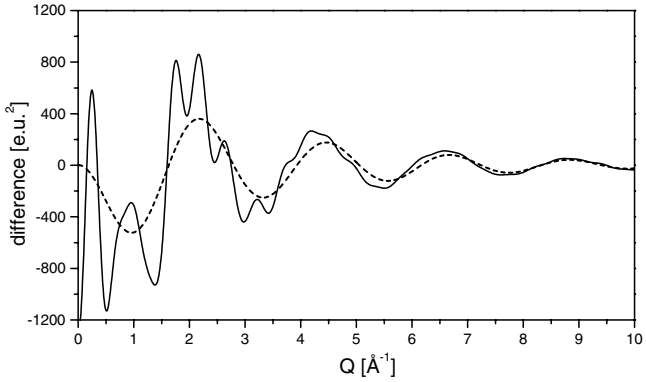

Figure 3. The calculated effect of the solvation cage change after excitation of the iodine into the expanded A/A′ state. The dashed curve marks the difference in scattering cross-section from the Debye term, whereas the full curve takes into account the change in the iodine–CCl_4 cross-correlation term as calculated from the MD data.

At high Q the simulation (full curve) follows closely the pure gas scattering (dashed curve), seen as a damped sinusoidal oscillation. By contrast, in the low-Q region modifications to the gas scattering occur. These are due to the changes occurring in the structure of the solvation cage, which reacts to the expansion of the I_2 molecule.

4. Conclusions

It has been demonstrated that the solvation structure of iodine (as a model for a range of small molecules) can be extracted from the cross-correlations in solution scattering. The experiments performed on chlorinated solvents agree well with MD simulations. This opens up a way to understand scattering experiments on reaction dynamics in solution. Scattering will allow us to obtain a much richer picture of the solute structural changes as well as the reaction of the surrounding solvent, which is known to strongly influence the photoreaction. In order to give a full description of laser experiments where a high energy density is absorbed in the solution, one has to model the changes in solvent–solvent correlation, which may be thermal expansion, propagating shock waves or vibrational heat transfer in the local surrounding of the solute molecules. Work is currently under way to find a description of these effects.

Acknowledgments

Discussions with S Bratos, J Als-Nielsen, S Techert and R Neutze and support from ESRF staff are acknowledged. This work was supported by the EU programme ‘Famto’.

References

[1] Ihee H *et al* 2001 *Science* **291** 458
[2] Neutze R *et al* 2001 *Phys. Rev. Lett.* **87** 195508-1
[3] Geis A *et al* 2001 *J. Lumin.* **94–95** 493
[4] Schotte F *et al* 2002 *Third-Generation Hard X-Ray Synchrotron Radiation Sources* ed D Mills (New York: Wiley)
[5] Plech A, Randler R, Geis A and Wulff M 2002 *J. Synchrotron Radiat.* **9** 287
[6] Warren B E 1990 *X-ray Diffraction* (New York: Dover) (reprint)

[7] Soper A K and Luzar A 1992 *J. Chem. Phys.* **97** 1320
[8] Roux B and Sanchez del Rio M 'DABAX: a Dynamics Database for x-ray Applications' http://www.esrf.fr/computing/scientific/dabax/ using data from
Cromer D T and Mann J B 1968 *Acta Crystallogr.* A **24** 321
[9] Hajdu F 1972 *Acta Crystallogr.* A **28** 250
Pálinkás G 1973 *Acta Crystallogr.* A **29** 10
[10] Bratos S, Vuilleumier R, Mirloup F and Wulff M 2002 *J. Chem. Phys.* **116** 10615
[11] Duffy E M, Severance D L and Jorgensen W L 1992 *J. Am. Chem. Soc.* **114** 7535
[12] Ferrario M and Evans M W 1982 *Chem. Phys.* **72** 141
[13] Nesbitt D J and Hynes J T 1982 *J. Chem. Phys.* **77** 2130
[14] Bergsma J P *et al* 1986 *J. Chem. Phys.* **84** 6151
[15] Ryckaert J P, Ciccotti G and Berendsen H J C 1977 *J. Comput. Phys.* **23** 327
[16] Harris A L, Berg M and Harris C B 1986 *J. Chem. Phys.* **84** 788
[17] Kelley D F, Abul-Haj N A and Jang D 1984 *J. Chem. Phys.* **80** 4105